European Radiology (2023) 33:1353–1363
https://doi.org/10.1007/s00330-022-09087-6

GASTROINTESTINAL

Prediction of tumor budding in patients with rectal adenocarcinoma using *b*-value threshold map

Fangying Chen[1] · Shaoting Zhang[1] · Xiaolu Ma[1] · Yukun Chen[1] · Zhen Wang[1] · Yan Zhu[2] · Chenguang Bai[2] · Caixia Fu[3] · Robert Grimm[4] · Chengwei Shao[1] · Jianping Lu[1] · Fu Shen[1] · Luguang Chen[1]

Received: 29 April 2022 / Revised: 28 July 2022 / Accepted: 4 August 2022 / Published online: 23 August 2022

Abstract

Objective To investigate the feasibility of *b*-value threshold ($b_{Threshold}$) map in preoperative evaluation of tumor budding (TB) in patients with locally advanced rectal cancer (LARC).

Methods Patients with LARC were enrolled and underwent diffusion-weighted imaging (DWI). Contrast-to-noise ratio (CNR) between the lesions and normal tissues was assessed using DWI and $b_{Threshold}$ maps. TB was counted and scored using hematoxylin and eosin staining. Reproducibility for the apparent diffusion coefficient (ADC), $b_{Threshold}$ values, and region-of-interest (ROI) sizes were compared. Differences in ADC and $b_{Threshold}$ values with low-intermediate and high TB grades and the correlations between mean ADC and $b_{Threshold}$ values with TB categories were analyzed. Diagnostic performance of ADC and $b_{Threshold}$ values was assessed using area under the curve (AUC) and decision curve analysis.

Results Fifty-one patients were evaluated. The CNR on $b_{Threshold}$ maps was significantly higher than that on DW images (9.807 ± 4.811 vs 7.779 ± 3.508, $p = 0.005$). Reproducibility was excellent for the ADC (ICC 0.933; CV 8.807%), $b_{Threshold}$ values (ICC 0.958; CV 7.399%), and ROI sizes (ICC 0.934; CV 8.425%). Significant negative correlations were observed between mean ADC values and TB grades and positive correlations were observed between mean $b_{Threshold}$ values and TB grades ($p < 0.05$). $b_{Threshold}$ maps showed better diagnostic performance than ADC maps (AUC, 0.914 vs 0.726; $p = 0.048$).

Conclusions In LARC patients, $b_{Threshold}$ values could distinguish different TB grades better than ADC values, and $b_{Threshold}$ maps may be a preoperative, non-invasive approach to evaluate TB grades.

Key Points

- *Compared with diffusion-weighted images, $b_{Threshold}$ maps improved visualization and detection of rectal tumors.*
- *Agreement and diagnostic performance of $b_{Threshold}$ values are superior to apparent diffusion coefficient in assessing tumor budding grades in patients with locally advanced rectal cancer.*
- *$b_{Threshold}$ maps could be used to evaluate tumor budding grades non-invasively before operation.*

Keywords Rectal cancer · Diffusion magnetic resonance imaging · Clinical pathology

Abbreviations

ADC	Apparent diffusion coefficient
$b_{Threshold}$	*b*-value threshold
CNR	Contrast-to-noise ratio
CRC	Colorectal cancer
DWI	Diffusion-weighted imaging
LARC	Locally advanced rectal cancer
MRI	Magnetic resonance imaging

Fangying Chen and Shaoting Zhang contributed equally.

✉ Fu Shen
ssff_53@163.com

✉ Luguang Chen
chen_lu_guang@sina.com

[1] Department of Radiology, Changhai Hospital, Naval Medical University, NO. 168 Changhai Road, Shanghai 200433, China

[2] Department of Pathology, Changhai Hospital, Shanghai, China

[3] MR Application Development, Siemens Shenzhen Magnetic Resonance Ltd, Shenzhen, China

[4] MR Applications Predevelopment, Siemens Healthineers Ltd., Erlangen, Germany

RC Rectal cancer
TB Tumor budding

Introduction

Colorectal cancer (CRC) is one of the most common digestive tumors and ranks the third cause in cancer mortality worldwide [1]. Rectal cancer (RC) accounts for approximately one-third of all CRC cases [2]. There is an increasing attention to the diagnosis, treatment, and prognosis of patients with RC. The appropriate treatment plan depends on the tumor-node-metastasis (TNM) staging system. However, patients with the same RC stage at initial diagnosis may have markedly different clinical outcomes [3–5]. Novel biomarkers are needed to explore and better stratify the clinical outcomes in RC patients.

Tumor budding (TB) presents as a single cell or a cell cluster of up to four tumor cells at the invasive margins of CRCs [6]. It is assessed by pathologists using the International Tumor Budding Consensus Conference (ITBCC) recommendations on hematoxylin and eosin (H&E) staining and scored by the budding count. TB is an independent adverse prognostic factor in CRC [7–10]. High-grade TB has been correlated with adverse clinicopathological features, including high TNM stage and poor overall and disease-free survival [6]. TB is included as a supplemental prognostic factor for CRC in the TNM (2017) and WHO (2019) classification schemes [11–13] and as a recommended element in the College of American Pathologists and International Collaboration on Cancer Reporting protocols for CRC histopathology [14]. TB potentially affects clinical decision-making for patients with locally advanced rectal cancer (LARC). High-grade TB is an adverse prognostic factor and is an indication for adjuvant chemotherapy in patients with stage II RC [7, 15]. However, clinical characteristics and tumor stages are poor predictors of tumor response to neoadjuvant chemoradiotherapy and overall prognosis [16, 17]. Moreover, TB is an indicator of metastasis and indicates a lack of response to neoadjuvant therapy if detected in pre-treatment biopsies [18–20]. Management and treatment strategies could be tailored for LARC patients who would benefit from adjuvant therapy or who are not likely to exhibit a complete pathological tumor response to neoadjuvant chemoradiotherapy. LARC biopsies are traumatic, and samples usually yield a small amount of tumor material. Thus, preoperative biomarkers of TB are of immense importance and would provide a non-invasive approach for the evaluation of TB.

Magnetic resonance imaging (MRI) is a non-invasive imaging technique and is widely used to evaluate preoperative staging and treatment response in patients with RC [21–24]. However, conventional MR images primarily provide qualitatively diagnostic information of RC lesions rather than quantitative metrics that reflect clinicopathologic information. Diffusion-weighted imaging (DWI) could evaluate the microscopic mobility of water molecules in lesions, and the derived apparent diffusion coefficient (ADC) values can be quantitatively evaluated and used to diagnose rectal tumors and evaluate the treatment response. With the increased amplitude of *b*-values, DWI images and ADC values are more sensitive to tumors than to normal tissues [24–26]. However, DWI images acquired with very high *b*-values result in significant image distortion and lower signal-to-noise ratios (SNR) [27, 28].

b-value threshold ($b_{\mathrm{Threshold}}$) map, derived from DWI images, has been proposed as a novel diffusion contrast method [29]. $b_{\mathrm{Threshold}}$ map provides improved lesion visualization for prostate, breast, and rectal tumors than conventional DWI images [23, 28] and improves the signal contrast between lesions and normal tissues. It might also compliment DWI and ADC in the evaluation of the pathologic features of RC [23].

The use of $b_{\mathrm{Threshold}}$ map for the preoperative evaluation of TB has not been assessed. This study investigated the preoperative use of $b_{\mathrm{Threshold}}$ maps to evaluate TB in LARC patients and to compare the diagnostic performance of $b_{\mathrm{Threshold}}$ maps with ADC maps in patients with different TB grades.

Materials and methods

Patients

The present study was approved by the local Institutional Review Board (Committee on Ethics of Biomedicine, Changhai Hospital of Shanghai). Informed consent was waived for this retrospective study. Between January 2018 and December 2020, 113 patients with LARC who underwent rectal MRI before surgical resection were considered for the study. Inclusion criteria were (1) pathologically confirmed rectal adenocarcinoma; (2) complete postoperative pathological data, including the TB grade; (3) and single focal lesion. The exclusion criteria were (1) any treatment (radiotherapy, chemotherapy, or chemoradiotherapy) prior to surgery; (2) more than 2 weeks between MRI and surgery; (3) poor quality DWI image; (4) simultaneous distant metastases; (5) and invasion of the circumferential resection margin. In all, 51 patients with LARC were included in the final study (Fig. 1). Clinical data and patient information were retrospectively retrieved from clinical and pathological databases, including gender, age, body mass index, pathological stage, TN stage, tumor location, differentiation, tumor deposit, lymphovascular invasion, perineural invasion, molecular biomarkers of the Ras signaling pathway (KRAS, NRAS, and BRAF types), CEA, CA19-9, and mismatch repair (MMR) status (deficient MMR and proficient MMR).

Magnetic resonance imaging

All rectal MRI was performed on a 3-Tesla MRI system (MAGNETOM Skyra, Siemens Healthcare GmbH) using an

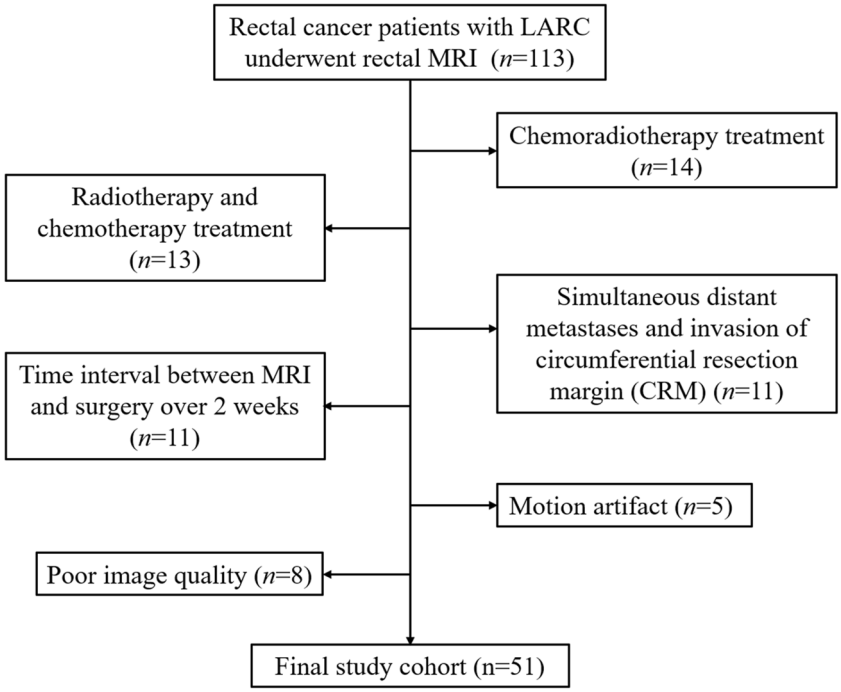

Fig. 1 Patient selection flow diagram

18-channel phased-array body coil and an integrated spine coil. Before scanning, intestinal cleaning was performed by enema administration using 20 mL of glycerin. The imaging protocol included sagittal T2-weighted imaging (T2WI), oblique axial high-resolution T2WI, axial DWI (the optimal *b*-value combination of 0 and 1000 s/mm^2 was recommended for RC based on previous studies [23, 30]), and axial T1-weighted imaging (T1WI). The main imaging parameters of the MRI protocol are summarized in supplemental Table 1. Gadolinium contrast-enhanced T1WI of the pelvis was obtained in the sagittal, coronal, and axial planes. The total scan time was approximately 10 min.

Image analysis

DWI images were independently evaluated by two experienced pelvic radiologists using a prototype post-processing software (Body Diffusion Toolbox, Siemens Healthcare GmbH). ADC maps were derived from DW images using the mono-exponential model

$$\mathrm{ADC} = 1/b * \log(S_0/S_\mathrm{b})$$

where S_0 and S_b represent the signal intensity with b = 0 s/mm^2 and with $b > 0$ s/mm^2 diffusion weighting, respectively. $b_\mathrm{Threshold}$ map was calculated using the formula

$$b_\mathrm{Threshold} = -1/\mathrm{ADC} * \log(\mathrm{Threshold}/S_0)$$

with *Threshold* defined as 50 au for RC, the intensities of $b_\mathrm{Threshold}$ map indicate the *b*-values at which the diffusion signal drops under a given threshold, and its unit is s/mm^2 [23, 28]. Single slices with the maximum cross-sectional tumor size were used to delineate the regions of interest (ROIs) and were manually outlined on ADC and $b_\mathrm{Threshold}$ maps of the lesions by two independent observers. The mean values of ADC and $b_\mathrm{Threshold}$ were recorded for each lesion (supplemental Fig. 1). In addition, the areas of ROI were also recorded. The contrast-to-noise ratios (CNRs) of the DWI images with b = 1000 s/mm^2 and $b_\mathrm{Threshold}$ maps were determined using

$$\mathrm{CNR} = \left|SI_{\text{lesion}} - SI_{\text{gluteus maximus}}\right| / \left(\sigma_{\text{lesion}}{}^2 + \sigma_{\text{gluteus maximus}}{}^2\right)^{1/2}$$

where *SI* and σ refer to the mean signal intensity and standard deviation of the ROI, respectively, of the lesion or gluteus maximus (same size = 100 voxels).

Pathological evaluation

All tissue sections underwent H&E staining. Histopathology results included tumor TN staging, histological grade, presence of perineural invasion, presence of lymph-vascular invasion (LVI), tumor deposits, and descriptions of the circumferential resection margins [21].

H&E-stained sections were scanned at medium power (10 × magnification), and an area with maximal budding was identified at the invasive front. TB was counted and scored by two experienced pathologists with consensus, according to the ITBCC 2016 Recommendations [31]. TB was counted in a selected area at 20 × magnification.

The bud count was divided by a normalization factor to determine the tumor bud count per 0.785 mm^2 [31]. TB categories were based on the bud count and defined as follows: Bd 1 (low-grade): 0–4 buds; Bd 2 (intermediate-grade): 5–9 buds; Bd 3 (high-grade): 10 buds or more. Patients were divided into two groups, low-intermediate (Bd 1+2) and high grade (Bd 3) for analysis.

Statistical analysis

SPSS (version 22.0, Inc.) and MedCalc Statistical software (version 13.0.0.0, MedCalc Software) were used to perform statistical analyses. The Kolmogorov-Smirnov test was used to check for the normality of continuous variables. Continuous variables are presented as mean and standard deviation or median and quartile according to the normal distribution of data, and categorical variables are expressed as percentages. Categorical variables were assessed using the chi-square test or Fisher's exact test. Interobserver reproducibility for the ADC, $b_{Threshold}$ values, and ROI sizes was assessed using intraclass correlation coefficients (ICCs), coefficients of variability (CVs), and Bland-Altman plots. ICC values > 0.75 indicated excellent agreement, 0.4 to 0.75 indicated good agreement, and < 0.4 indicated poor agreement. Levene's test was used to test for equality of error variances. Significant differences in CNR between DWI (b = 1000 s/mm^2) images and $b_{Threshold}$ maps were assessed using paired-sample t-tests. The ADC and $b_{Threshold}$ values of the two radiologists were averaged. The correlations of the mean ADC and $b_{Threshold}$ values with TB category were determined using Spearman's rank correlation test. Differences in ADC and $b_{Threshold}$ values among Bd grades 1, 2, and 3 were evaluated using Kruskal-Wallis one-way ANOVA with a pairwise multiple comparisons test. Differences in ADC and $b_{Threshold}$ values between budding groups Bd 1+2 and Bd 3 were evaluated using the Mann-Whitney U test. The diagnostic performance of the ADC and $b_{Threshold}$ values for group Bd 1+2 vs group Bd 3 was assessed using area under the curve (AUC) and compared using the DeLong test. The decision curve analysis (DCA) was performed by estimating the net benefit with probability thresholds to confirm the clinical benefit. A p value < 0.05 indicated statistical significance.

Results

Patient characteristics

A total of 51 LARC patients with rectal adenocarcinomas were enrolled in the final analysis, including 32 males with a mean age of 56.3 ± 8.8 years (range 32–74 years). Total mesorectal excision was performed at a time interval of 7.8 ± 4.3 days (range 3–14 days) after MR imaging. There were 13 Bd 1, 13 Bd 2, and 25 Bd 3 patients. No case had a positive circumferential resection margin. Characteristics and pathological outcomes were not significantly different among the patients (Table 1).

All 51 cases of LARC had a single lesion, of which 29 cases had space-occupying masses, 16 cases had an irregular thickening of the local intestinal wall, and 6 cases had abnormal local nodular signals. All lesions demonstrated high signals on DWI images with b = 1000 s/mm^2 and on $b_{Threshold}$ maps (Fig. 2). Significant differences were observed in CNR between DWI images and $b_{Threshold}$ maps (7.779 ± 3.508 vs 9.807 ± 4.811, p = 0.005).

Interobserver variability of ADC, $b_{Threshold}$ values, and ROI sizes

There was an excellent reproducibility for ADC (ICC, 0.933; CV, 8.807%) and $b_{Threshold}$ measurements (ICC, 0.958; CV, 7.399%). In addition, the bias and limits of agreement for ADC (−2.655%; −21.666 to 16.356) and $b_{Threshold}$ (3.880%; −16.788 to 24.549) were relatively low (Table 2, Fig. 3). No significant difference was observed between the two observers in ROI size delineation (365.2 ± 159.5 mm^2 vs 375.1 ± 168.5 mm^2, p = 0.491), which also had excellent agreement, with ICC and CV values of 0.934 and 8.425%, respectively (Table 2).

Correlation and comparison of mean ADC and $b_{Threshold}$ values among and between different TB grades

For patients with LARC, a significant negative correlation was observed between mean ADC values and TB grades, and a positive correlation was found between mean $b_{Threshold}$ values and TB grades. Categories Bd 1, 2, and 3 had Spearman correlation coefficients of −0.392 and 0.675 (p < 0.05) for ADC and $b_{Threshold}$, respectively. Significant differences were observed in mean ADC and $b_{Threshold}$ values among Bd categories 1, 2, and 3 and between the groups Bd 1+2 and Bd 3, respectively (Table 3). Multiple pairwise comparisons showed that significant differences were found in ADC and $b_{Threshold}$ values between categories Bd 1 and Bd 3 and between categories Bd 2 and Bd 3. No significant differences were found in ADC and $b_{Threshold}$ values between categories Bd 1 and Bd 2. The mean $b_{Threshold}$ value of category Bd3 was significantly higher than the Bd 1+2 group (Fig. 4, supplemental Table 2) (p < 0.05).

Diagnostic performance of ADC and $b_{Threshold}$

The AUC, sensitivity, and specificity of the mean ADC and $b_{Threshold}$ values for differentiating groups Bd 1+2 vs Bd 3

Table 1 Patient demographics and clinicopathologic findings

Variables	Tumor budding grade		*p* value
	Low-intermediate (*n* = 26)	High (*n* = 25)	
Gender (male/female)	16/10	16/9	.86
Age (years)	56.9 ± 8.2	55.0 ± 10.4	.47
BMI (kg/m^2)	24.1 ± 3.2	23.8 ± 3.4	.75
Pathological stage, *n* (%)			.12
II	16 (61.5)	10 (40.0)	
III	10 (38.5)	15 (60.0)	
Pathological T stage, *n* (%)			.24
T1–2	9 (34.6)	5 (20.0)	
T3–4	17 (65.4)	20 (80.0)	
Pathological N stage, *n* (%)			.12
N0	16 (61.5)	10 (40.0)	
N1–2	10 (38.5)	15 (60.0)	
Tumor location, *n* (%)			.79
Upper	5 (19.2)	6 (24.0)	
Middle	17 (65.4)	14 (56.0)	
Lower	4 (15.4)	5 (20.0)	
Differentiation, *n* (%)			> 0.99
Well	4 (15.4)	3 (12.0)	
Moderate	13 (50.0)	14 (56.0)	
Poor	9 (34.6)	8 (32.0)	
Tumor deposit, *n* (%)			.69
No	17 (65.4)	15 (60.0)	
Yes	9 (34.6)	10 (40.0)	
Lymphovascular invasion, *n* (%)			.49
No	19 (73.1)	16 (64.0)	
Yes	7 (26.9)	9 (36.0)	
Perineural invasion, *n* (%)			.87
No	15 (57.7)	15 (60.0)	
Yes	11 (42.3)	10 (40.0)	
KRAS type, *n* (%)			.33
Wild	18 (69.2)	14 (56.0)	
Mutant	8 (30.8)	11 (44.0)	
NRAS type, *n* (%)			.69
Wild	16 (61.5)	14 (56.0)	
Mutant	10 (38.5)	11 (44.0)	
BRAF type, *n* (%)			.69
Wild	18 (69.2)	16 (64.0)	
Mutant	8 (30.8)	9 (36.0)	
CEA* (ng/mL), *n* (%)			.32
< 5	19 (73.1)	15 (60.0)	
≥ 5	7 (26.9)	10 (40.0)	
CA19-9* (U/mL), *n* (%)			.48
< 37	20 (76.9)	17 (68.0)	
≥ 37	6 (23.1)	8 (32.0)	
MMR status, *n* (%)			.35
dMMR	1 (3.8)	3 (12.0)	
pMMR	25 (96.2)	22 (88.0)	

BMI, body mass index; BRAF; *CA19-9*, carbohydrate antigen 19-9; *CEA*, carcinoembryonic antigen; *dMMR*, deficient mismatch repair; KRAS; NRAS; *pMMR*, proficient mismatch repair. * Postoperative blood samples

were 0.726, 69.2%, and 84.0% and 0.914, 88.5%, and 92.0%, respectively (Table 4). The diagnostic performance of $b_{Threshold}$ maps was greater than that of ADC values for group Bd 1+2 vs group 3 ($p = 0.048$) and the optimal cut-off threshold of $b_{Threshold}$ values was 1.773×10^3 s/mm^2 (Fig. 5 and supplemental Fig. 2).

Decision curve analysis

The DCA showed an adequate performance for ADC and $b_{Threshold}$ values in distinguishing group Bd 1+2 from group Bd 3 (Fig. 6). When the threshold probability was between 0.15 and 1.0, the $b_{Threshold}$ map for predicting category Bd

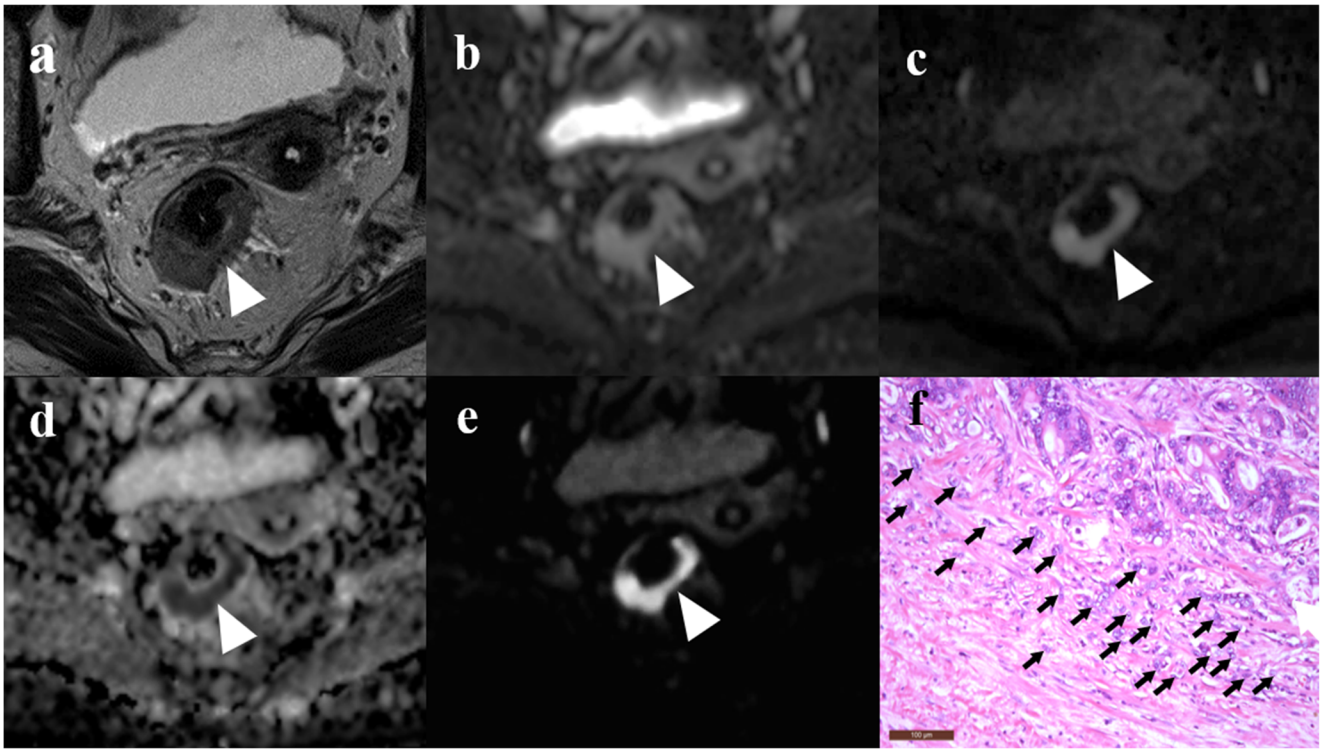

Fig. 2 Images of a rectal cancer lesion from a patient with poorly differentiated adenocarcinoma confirmed as stage IIa (pT3N0). **a** T2WI showing abnormal signals on the posterior of the rectal wall (arrow). **b** Axial DWI at $b = 0$ s/mm^2 showing abnormal signals on the posterior of the rectal wall (arrow). **c** DWI at $b = 1000$ s/mm^2 showing the lesion with high-signal intensity (arrow). **d** ADC map showing the lesion with low-signal intensity (arrow). **e** The $b_{Threshold}$ map showing the lesion with high-signal intensity (arrow). **f** Hematoxylin & eosin (H&E)–stained high-grade histopathological section showing more than 10 buds at the invasive front (black arrows)

3 TB showed a greater advantage than either the "all" or "none" scheme.

Discussion

TB is used as a prognostic biomarker for solid tumors such as RC and has the potential to stratify patients for different therapeutic options [32, 33]. TB is closely related to many different clinical and histological parameters, including histological grade, lymph node involvement, and lymphovascular invasion and metastasis in RC [34–39]. High-grade TB predicts adverse outcomes in LARC, including higher TNM stages, higher recurrence rates, and increased risk of mortality [34–39]. Identifying individuals with high-grade TB in a preoperative assessment could be helpful for guiding clinical practice.

We explored the values of ADC and $b_{Threshold}$ in the preoperative diagnosis of TB. We found that significant correlations and differences were observed in mean ADC and $b_{Threshold}$ values between different categories of TB grades, particularly group Bd 1+2 vs group Bd 3. The diagnostic

Table 2 Interobserver variability of ADC and $b_{Threshold}$ values

Parameters	Observers	Variable value	ICC (95% CI)	CV (%)	Bias (%, ± 1.96 SD)
ADC[a] ($\times 10^{-3}$ mm^2/s)	#1 #2	0.898 (0.779 to 1.053) 0.924 (0.783 to 1.105)	0.933 (0.882 to 0.961)	8.807	−2.655 (−21.666 to 16.356)
$b_{Threshold}$[a] ($\times 10^3$ s/mm^2)	#1 #2	1.859 (1.623 to 2.176) 1.809 (1.450 to 2.166)	0.958 (1.151 to 1.761)	7.399	3.880 (−16.788 to 24.549)
ROI size[b] (mm^2)	#1 #2	365.2 ± 159.5 375.1 ± 168.5	0.934 (0.885 to 0.962)	8.425	−2.718 (−21.303 to 15.867)

[a] Data are presented as median (interquartile range); [b] data are presented as mean ± standard deviation; *CI*, confidence interval; *CV*, coefficient of variation; *ICC*, intraclass correlation coefficient; *ROI*, region-of-interest; *SD*, standard deviation

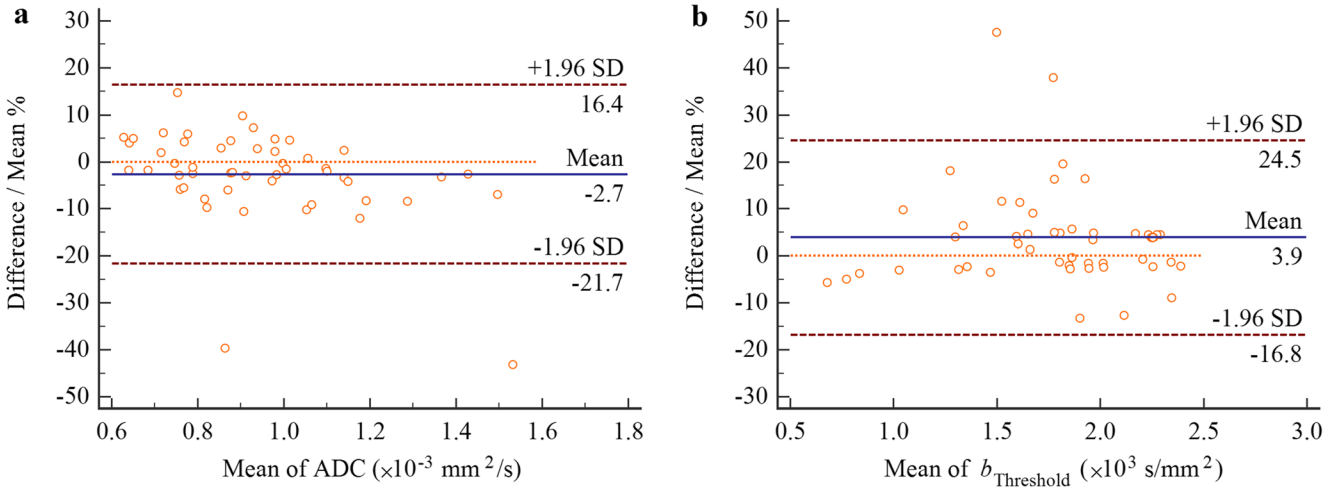

Fig. 3 Bland-Altman plots. **a** ADC plot. **b** $b_{Threshold}$ plot. The solid blue line in each plot indicates the mean difference in reads between two radiologists. The dashed red lines indicate the limits of the agreements

performance of $b_{Threshold}$ maps was higher than those of ADC and may be applicable in the preoperative TB evaluation in LARC patients.

The present study showed that the ADC value for patients in the Bd 1+2 group was significantly higher than that for patients in the Bd 3 group. In contrast, we found that the mean $b_{Threshold}$ value for patients in the Bd 3 group was significantly higher than that in Bd 1+2 group. This finding could be explained by Bd 3 tumors having more tumor cells at the invasive margin with higher cell density and smaller interstitium. ROC curves for ADC and $b_{Threshold}$ showed large AUCs (> 0.7), indicating that both values may be used to distinguish patients in the Bd 3 group from patients in the Bd 1+2 group.

We performed DCA to assess the performance of ADC and $b_{Threshold}$ values in distinguishing the Bd 1+2 group from the Bd 3 group. The net benefit of $b_{Threshold}$ maps was better than those of ADC and had threshold probabilities of 0.15–1.0. We found that $b_{Threshold}$ values can distinguish between Bd 1 patients from Bd 3 patients, and Bd 2 patients from Bd 3 patients. However, ADC values can only distinguish Bd 1 patients from Bd 3 patients, indicating that $b_{Threshold}$ maps are better for preoperative prognosis of TB for LARC patients. The underlying mechanism of $b_{Threshold}$ values outperform ADC may be explained as follows: Firstly, $b_{Threshold}$ maps offer a positive contrast in dense tissues which more conform to the doctor's viewing habits, while the ADC maps show a negative contrast in dense lesions. Secondly, the signal intensities of $b_{Threshold}$ maps represent *b*-values at which the diffusion signal drops under a given threshold [29]. In the present study, 50 a.u. was optimized and used for evaluating rectal lesions. Compared with ADC, it has large dynamical range on $b_{Threshold}$ maps among different Bd grades. Thirdly, the values of $b_{Threshold}$ maps among budding grades 1, 2, and 3 were 1.508 (1.151–1.761), 1.547 (1.361–1.634), and 1.982 (1.844–2.057) $\times 10^3$ s/mm^2, respectively. Those maps have some similarity to DWI images acquired with high *b*-values of 1500–2000 s/mm^2; however, ADC map was derived from relatively low *b*-values of 0 and 1000 s/mm^2. Therefore, better lesion-to-normal tissue contrast was obtained using $b_{Threshold}$ maps, as well as improved diagnostic performance in differentiating TB grades (Bd 1+2 vs Bd 3).

Table 3 Comparison of tumor budding category in RC patients using DWI parameters

Parameters	TB category			*p* value	TB category		*p* value
	Bd 1 (*n* = 13)	Bd 2 (*n* = 13)	Bd 3 (*n* = 25)		Bd 1+2 (*n* = 26)	Bd 3 (*n* = 25)	
ADC* ($\times 10^{-3}$ mm^2/s)	1.128 (0.724–1.235)	1.011 (0.939–1.058)	0.784 (0.748–0.916)	.020	1.015 (0.911–1.128)	0.784 (0.748–0.916)	.006
$b_{Threshold}$* ($\times 10^3$ s/mm^2)	1.508 (1.151–1.761)	1.547 (1.361–1.634)	1.982 (1.844–2.057)	< .001	1.533 (1.156–1.734)	1.982 (1.844–2.057)	< .001

*Parameters are presented as median and interquartile range. *Bd*, budding; *TB*, tumor budding

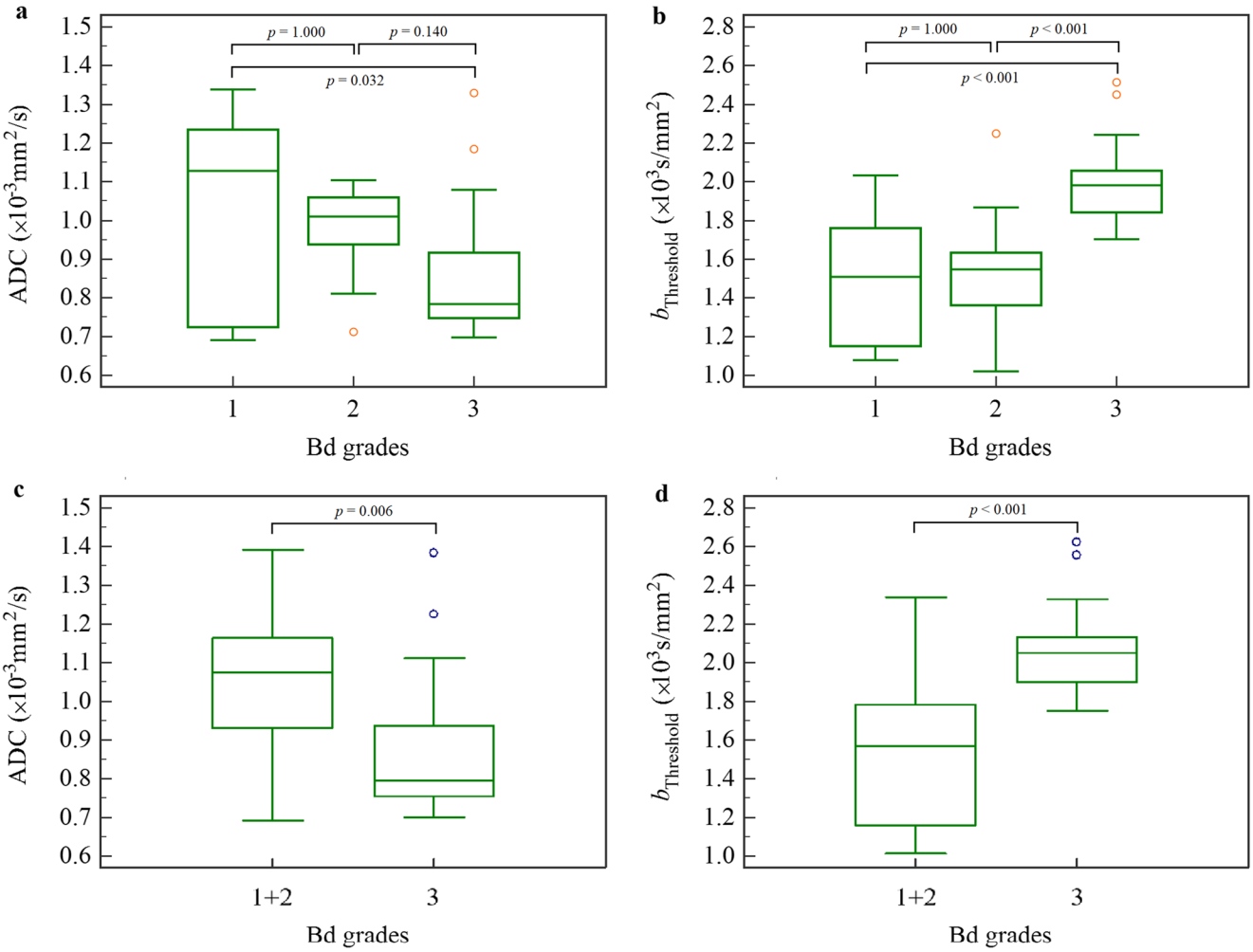

Fig. 4 Box plots of (**a**) apparent diffusion coefficient (ADC) and (**b**) $b_{Threshold}$ values in Bd groups 1, 2, and 3. Box plots of (**c**) apparent diffusion coefficient (ADC) and (**d**) $b_{Threshold}$ values in low-intermediate grade and high-grade TB

Table 4 Diagnostic performance of ADC and $b_{Threshold}$ values in differentiating TB grades (Bd 1+2 vs Bd 3)

	ADCa	$b_{Threshold}$ [b]
AUC*	0.726	0.914
95% CI	0.574–0.878	0.823–0.999
Cut-off value	0.956	1.773
Sensitivity (%)	0.692	0.885
Specificity (%)	0.840	0.920
Accuracy (%)	0.765	0.902
PLR	4.327	11.058
NLR	0.366	0.125
PPV (%)	0.818	0.920
NPV (%)	0.724	0.885

Bd, budding; *NLR*, negative likelihood ratio; *NPV*, negative predictive value; *PLR*, positive likelihood ratio; *PPV*, positive predictive value

[a] $\times 10^{-3}$ mm^2/s; [b] $\times 10^3$ s/mm^2

*DeLong test, significant difference was observed in AUC between ADC and $b_{Threshold}$ values in differentiating TB grades ($p = 0.048$)

We found that $b_{Threshold}$ maps provided higher CNRs and improved visualization and detection of lesions compared with DWI images. This is consistent with observations that $b_{Threshold}$ maps provide better lesion visualizations for rectal tumors [23, 27, 28]. Rectal tumors show hyperintensity in $b_{Threshold}$ maps in comparison with normal tissues, which are more familiar to physicians [23]. We found that $b_{Threshold}$ maps significantly improve the signal contrast between lesions and normal tissue and provided significantly higher CNR than DWI images with a b = 1000 s/mm^2. RC lesions often are irregularly shaped and cannot be easily distinguished from the surrounding adipose tissues due to inflammation and blood vessel invasion. The signal contrast of $b_{Threshold}$ maps helps to detect such lesions [40]. Improved CNR would also allow for more accurate ROIs for quantitative measurements. Apart from the definition and a standardized scoring system, the application of TB has been hindered by the lack of reproducibility. Puppa G found that the reproducibility assessment of TB is higher in early colorectal cancer and experienced

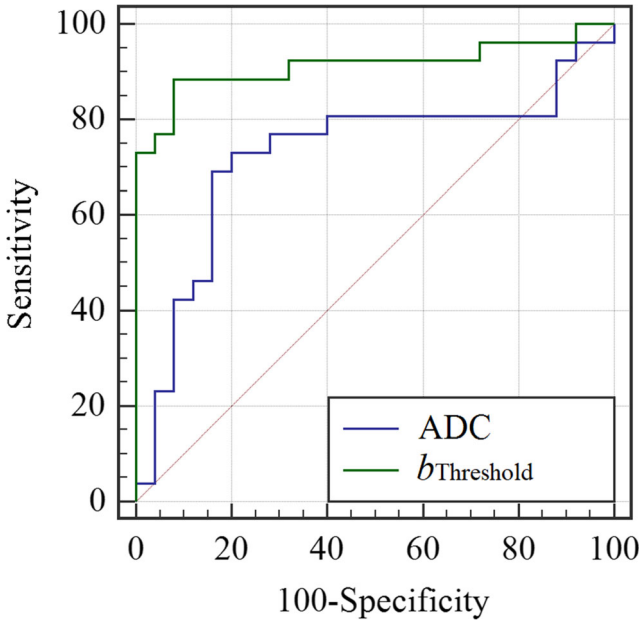

Fig. 5 Receiver operating characteristic curves of the ADC and $b_{Threshold}$ values for differentiating tumor budding (Bds 1+2 and 3). Areas under the curves of ADC and $b_{Threshold}$ values are 0.726 and 0.914, respectively (p = 0.048)

gastrointestinal pathologists [41]. Immunohistochemistry (IHC) highlights tumor budding cells and improves the visualization of TBs [42–45] and the reproducibility. Our study demonstrated that $b_{Threshold}$ maps could be used to evaluate the TB grades preoperatively in patients with LARC, showing excellent reproducibility among $b_{Threshold}$ values (ICC 0.958; CV 7.399%). Narrow intervals observed in Bland-Altman plots indicated that interobserver variability would be low in clinical use. No complex post-processing technique is needed to assess TB using $b_{Threshold}$ maps with a given optimized b value. By quantifying the optimal cut-off threshold, less time would be needed to perform the complex diagnosis (e.g., high TB grades have $b_{Threshold}$ values > 1.773).

There were several limitations in this study. First, a small number of patients were enrolled in our retrospective study, making the study prone to selection bias. The small sample and retrospective nature of the study may explain the lack of predictive value of TB grades for lymph node positivity in this cohort. Second, it was a single-center study with only one MRI system. Finally, our final budding count in this work was based on H&E assessments as per the ITBCC group recommendations. Despite IHC's potential usefulness in effectively confirming bud count in challenging cases, the H&E method is more cost-effective and can reduce the economic burden of patients. Large multicenter randomized controlled trials assessing $b_{Threshold}$ maps that also compare the effectiveness of H&E staining with IHC are necessary to validate our results and provide additional information.

In conclusion, $b_{Threshold}$ maps may serve as a preoperative non-invasive alternative for evaluating TB in patients with LARC. $b_{Threshold}$ values could distinguish among different TB grades in LARC patients due to their higher CNR. TB grades based on $b_{Threshold}$ values could be considered along with adverse clinicopathological parameters in LARC patients when assessing individualized therapeutic strategies.

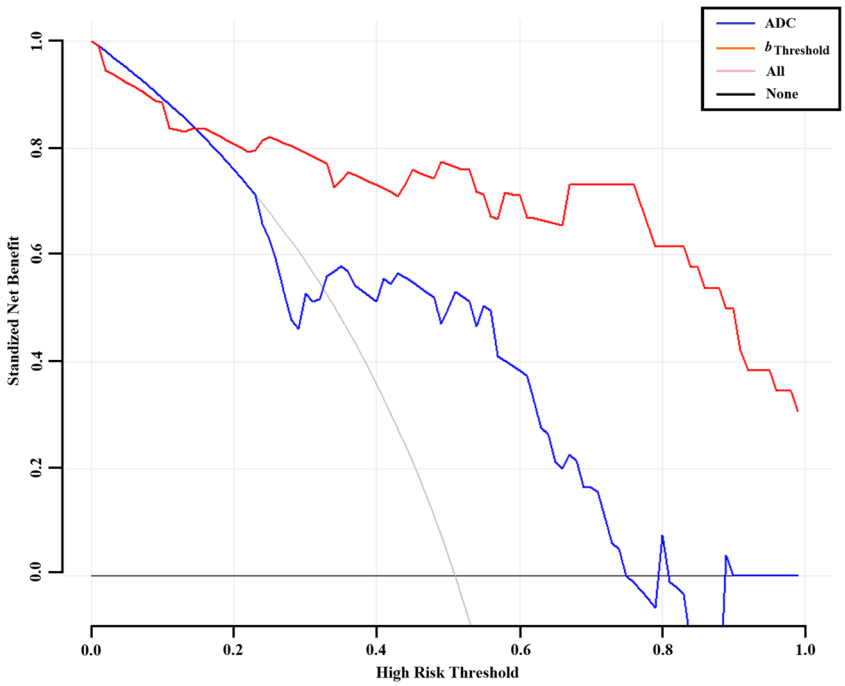

Fig. 6 Decision curve analysis of the apparent diffusion coefficient (ADC) and $b_{Threshold}$ values. The light gray line represents the assumption that all patients had high-grade TB. The dark gray line represents the hypothesis that no patients were high-grade TB. The red decision curve shows that when the threshold probability was between 0.15 and 1.0, the $b_{Threshold}$ value was better in predicting high-grade TB than the ADC value

Supplementary Information The online version contains supplementary material available at https://doi.org/10.1007/s00330-022-09087-6.

Funding This study has received funding by the National Key Clinical Specialist Construction Programs of China (Grant Number N/A); Youth Initiative Fund of Naval Medical University (Grant Number 2018QN05), and Natural Science Foundation of Shanghai (Grant Number 20ZR1456300).

Declarations

Guarantor The scientific guarantor of this publication is Luguang Chen.

Conflict of interest Two coauthors (Caixia Fu and Robert Grimm) are employees of Siemens Healthcare, and they declared that they have no conflict of interest.

Statistics and biometry No complex statistical methods were necessary for this paper.

Informed consent Written informed consent was waived by the Institutional Review Board.

Ethical approval Institutional Review Board approval was obtained.

Study subjects or cohorts overlap Twenty-nine patients with pathologically proven as T2 or T3, had been partially reported in our previous study, were included and we further enlarged the sample size in the present study. Previous work mainly aimed to investigate the usefulness of *b*-value threshold ($b_{Threshold}$) map in the evaluation of rectal adenocarcinoma by comparing it with diffusion-weighted images and ADC maps regarding lesion detection and the prediction of pathological features, which found that compared with DWI, the $b_{Threshold}$ map offers significantly higher CNR, which improves lesion visualization and detection. $b_{Threshold}$ values could differentiate between pathologic differentiation degrees and T stages and have a better diagnostic performance than ADC for N staging, while several reports showed that tumor budding (TB) is an indicator of metastasis and adverse reaction to neoadjuvant therapy in colorectal cancers, which help assess individualized therapeutic strategies. However, a preoperative and non-invasive approach to evaluate TB grades is lacking. Therefore, the purpose of the current study was to investigate the feasibility of $b_{Threshold}$ maps in preoperative evaluations of TB in patients with locally advanced rectal cancer (LARC), which found $b_{Threshold}$ values could distinguish different TB grades better than ADC values in LARC patients, and $b_{Threshold}$ maps may be a preoperative, non-invasive approach to evaluate TB grades.

Methodology
- retrospective
- diagnostic or prognostic study
- performed at one institution

References

1. Siegel RL, Miller KD, Jemal A (2020) Cancer statistics, 2020. CA Cancer J Clin 70:7–30
2. Siegel RL, Miller KD, Sauer AG et al (2020) Colorectal cancer statistics, 2020. CA Cancer J Clin 70:145–164
3. Merkel S, Mansmann U, Papadopoulos T, Wittekind C, Hohenberger W, Hermanek P (2001) The prognostic inhomogeneity of colorectal carcinomas Stage III: a proposal for subdivision of Stage III. Cancer 92:2754–2759
4. Nagtegaal ID, Gosens MJ, Marijnen CA, Rutten HJ, van de Velde CJ, van Krieken JH (2007) Combinations of tumor and treatment parameters are more discriminative for prognosis than the present TNM system in rectal cancer. J Clin Oncol 25:1647–1650
5. Edge SB, Compton CC (2010) The American Joint Committee on Cancer: the 7th edition of the AJCC cancer staging manual and the future of TNM. Ann Surg Oncol 17:1471–1474
6. Dawson H, Galuppini F, Träger P et al (2019) Validation of the International Tumor Budding Consensus Conference 2016 recommendations on tumor budding in stage I-IV colorectal cancer. Hum Pathol 85:145–151
7. Rogers AC, Winter DC, Heeney A et al (2016) Systematic review and meta-analysis of the impact of tumour budding in colorectal cancer. Br J Cancer 115:831–840
8. Ueno H, Hase K, Hashiguchi Y et al (2014) Novel risk factors for lymph node metastasis in early invasive colorectal cancer: a multi-institution pathology review. J Gastroenterol 49:1314–1323
9. Petrelli F, Pezzica E, Cabiddu M et al (2015) Tumour budding and survival in stage II colorectal cancer: a systematic review and pooled analysis. J Gastrointest Cancer 46:212–218
10. Nakamura T, Mitomi H, Kanazawa H, Ohkura Y, Watanabe M (2008) Tumor budding as an index to identify high-risk patients with stage II colon cancer. Dis Colon Rectum 51:568–572
11. Bach AG (2017) TNM classification of malignant tumours. Radiologe 57:244–245
12. Doescher J, Veit JA, Hoffmann TK (2017) The 8th edition of the AJCC Cancer Staging Manual. HNO 65:956–961
13. Nagtegaal ID, Odze RD, Klimstra D et al (2020) The 2019 WHO classification of tumours of the digestive system. Histopathology 76:182–188
14. Lugli A, Zlobec I, Berger MD, Kirsch R, Nagtegaal ID (2021) Tumour budding in solid cancers. Nat Rev Clin Oncol 18:101–115
15. Betge J, Kornprat P, Pollheimer MJ et al (2012) Tumor budding is an independent predictor of outcome in AJCC/UICC stage II colorectal cancer. Ann Surg Oncol 19:3706–3712
16. Quah HM, Chou JF, Gonen M et al (2008) Pathologic stage is most prognostic of disease-free survival in locally advanced rectal cancer patients after preoperative chemoradiation. Cancer 113:57–64
17. Puppa G, Sonzogni A, Colombari R et al (2010) TNM staging system of colorectal carcinoma: a critical appraisal of challenging issues. Arch Pathol Lab Med 134:837–852
18. Zlobec I, Hädrich M, Dawson H et al (2014) Intratumoural budding (ITB) in preoperative biopsies predicts the presence of lymph node and distant metastases in colon and rectal cancer patients. Br J Cancer 110:1008–1013
19. Giger OT, Comtesse SC, Lugli A, Zlobec I, Kurrer MO (2012) Intra-tumoral budding in preoperative biopsy specimens predicts lymph node and distant metastasis in patients with colorectal cancer. Mod Pathol 25:1048–1053
20. Rogers AC, Gibbons D, Hanly AM et al (2014) Prognostic significance of tumor budding in rectal cancer biopsies before neoadjuvant therapy. Mod Pathol 27:156–162
21. Benson AB, Venook AP, Al-Hawary MM et al (2018) Rectal cancer, version 2.2018, NCCN clinical practice guidelines in oncology. J Natl Compr Canc Netw 16:874–901
22. Lambregts DMJ, van Heeswijk MM, Delli Pizzi A et al (2017) Diffusion-weighted MRI to assess response to chemoradiotherapy in rectal cancer: main interpretation pitfalls and their use for teaching. Eur Radiol 27:4445–4454

23. Shen F, Chen L, Li Z et al (2020) The usefulness of b value threshold map in the evaluation of rectal adenocarcinoma. Abdom Radiol (NY) 45:332–341
24. Iannicelli E, Di Pietropaolo M, Pilozzi E et al (2016) Value of diffusion-weighted MRI and apparent diffusion coefficient measurements for predicting the response of locally advanced rectal cancer to neoadjuvant chemoradiotherapy. Abdom Radiol (NY) 41:1906–1917
25. Bassaneze T, Gonçalves JE, Faria JF, Palma RT, Waisberg J (2017) Quantitative aspects of diffusion-weighted magnetic resonance imaging in rectal cancer response to neoadjuvant therapy. Radiol Oncol 51:270–276
26. Sun Y, Tong T, Cai S, Bi R, Xin C, Gu Y (2014) Apparent diffusion coefficient (ADC) value: a potential imaging biomarker that reflects the biological features of rectal cancer. PLoS One 9:e109371
27. Porter DA, Heidemann RM (2009) High resolution diffusion-weighted imaging using readout-segmented echo-planar imaging, parallel imaging and a two-dimensional navigator-based reacquisition. Magn Reson Med 62:468–475
28. Zhao N, Ma C, Ye X et al (2019) The feasibility of b-value maps based on threshold DWI for detection of breast cancer: a case-control STROBE compliant study. Medicine (Baltimore) 98: e17640
29. Gall P, Kasibhatla R, Meyer H (2014) Improved lesion visualization using B-value maps based on thresholded DWI images. Proc Intl Soc Mag Reson Med 22:2177
30. Chen L, Shen F, Li Z et al (2018) Diffusion-weighted imaging of rectal cancer on repeatability and cancer characterization: an effect of b-value distribution study. Cancer Imaging 18:43
31. Lugli A, Kirsch R, Ajioka Y et al (2017) Recommendations for reporting tumor budding in colorectal cancer based on the International Tumor Budding Consensus Conference (ITBCC) 2016. Mod Pathol 30:1299–1311
32. Mitrovic B, Schaeffer DF, Riddell RH, Kirsch R (2012) Tumor budding in colorectal carcinoma: time to take notice. Mod Pathol 25:1315–1325
33. Lugli A, Karamitopoulou E, Zlobec I (2012) Tumour budding: a promising parameter in colorectal cancer. Br J Cancer 106:1713–1717
34. Okuyama T, Nakamura T, Yamaguchi M (2003) Budding is useful to select high-risk patients in stage II well-differentiated or moderately differentiated colon adenocarcinoma. Dis Colon Rectum 46: 1400–1406
35. Choi HJ, Park KJ, Shin JS, Roh MS, Kwon HC, Lee HS (2007) Tumor budding as a prognostic marker in stage-III rectal carcinoma. Int J Colorectal Dis 22:863–868
36. Guzińska-Ustymowicz K (2005) The role of tumour budding at the front of invasion and recurrence of rectal carcinoma. Anticancer Res 25:1269–1272
37. Syk E, Lenander C, Nilsson PJ, Rubio CA, Glimelius B (2011) Tumour budding correlates with local recurrence of rectal cancer. Colorectal Dis 13:255–262
38. Sert Bektaş S, Inan Mamak G, Cırış IM, Bozkurt KK, Kapucuoğlu N (2012) Tumor budding in colorectal carcinomas. Turk Patoloji Derg 28:61–66
39. Wang LM, Kevans D, Mulcahy H et al (2009) Tumor budding is a strong and reproducible prognostic marker in T3N0 colorectal cancer. Am J Surg Pathol 33:134–141
40. Nougaret S, Reinhold C, Mikhael HW, Rouanet P, Bibeau F, Brown G (2013) The use of MR imaging in treatment planning for patients with rectal carcinoma: have you checked the "DISTANCE"? Radiology 268:330–344
41. Puppa G, Senore C, Sheahan K et al (2012) Diagnostic reproducibility of tumour budding in colorectal cancer: a multicentre, multinational study using virtual microscopy. Histopathology 61:562–575
42. Ueno H, Mochizuki H, Shinto E, Hashiguchi Y, Hase K, Talbot IC (2002) Histologic indices in biopsy specimens for estimating the probability of extended local spread in patients with rectal carcinoma. Cancer 94:2882–2891
43. Rieger G, Koelzer VH, Dawson HE et al (2017) Comprehensive assessment of tumour budding by cytokeratin staining in colorectal cancer. Histopathology 70:1044–1051
44. Kai K, Aishima S, Aoki S et al (2016) Cytokeratin immunohistochemistry improves interobserver variability between unskilled pathologists in the evaluation of tumor budding in T1 colorectal cancer. Pathol Int 66:75–82
45. Suzuki A, Togashi K, Nokubi M et al (2009) Evaluation of venous invasion by Elastica van Gieson stain and tumor budding predicts local and distant metastases in patients with T1 stage colorectal cancer. Am J Surg Pathol 33:1601–1607